A Voltage-dependent Persistent Sodium Current in Mammalian Hippocampal Neurons

C. R. French, P. Sah, K. J. Buckett, and P. W. Gage

From the John Curtin School of Medical Research, Australian National University, Canberra 2601, Australia

ABSTRACT   Currents generated by depolarizing voltage pulses were recorded in neurons from the pyramidal cell layer of the CA1 region of rat or guinea pig hippocampus with single electrode voltage-clamp or tight-seal whole-cell voltage-clamp techniques. In neurons in situ in slices, and in dissociated neurons, subtraction of currents generated by identical depolarizing voltage pulses before and after exposure to tetrodotoxin revealed a small, persistent current after the transient current. These currents could also be recorded directly in dissociated neurons in which other ionic currents were effectively suppressed. It was concluded that the persistent current was carried by sodium ions because it was blocked by TTX, decreased in amplitude when extracellular sodium concentration was reduced, and was not blocked by cadmium. The amplitude of the persistent sodium current varied with clamp potential, being detectable at potentials as negative as -70 mV and reaching a maximum at ~ -40 mV. The maximum amplitude at -40 mV in 21 cells in slices was -0.34 ± 0.05 nA (mean $\pm$ 1 SEM) and -0.21 ± 0.05 nA in 10 dissociated neurons. Persistent sodium conductance increased sigmoidally with a potential between -70 and -30 mV and could be fitted with the Boltzmann equation, $g = g_{max}/\{1 + \exp[(V' - V)/k)]\}$. The average g_{max} was 7.8 $\pm$ 1.1 nS in the 21 neurons in slices and 4.4 $\pm$ 1.6 nS in the 10 dissociated cells that had lost their processes indicating that the channels responsible are probably most densely aggregated on or close to the soma. The half-maximum conductance occurred close to -50 mV, both in neurons in slices and in dissociated neurons, and the slope factor (k) was 5–9 mV. The persistent sodium current was much more resistant to inactivation by depolarization than the transient current and could be recorded at >50% of its normal amplitude when the transient current was completely inactivated.

Because the persistent sodium current activates at potentials close to the resting membrane potential and is very resistant to inactivation, it probably plays an important role in the repetitive firing of action potentials caused by prolonged

depolarizations such as those that occur during barrages of synaptic inputs into these cells.

INTRODUCTION

In addition to the well-described transient sodium current that is activated by depolarization, inactivates rapidly, and is responsible for action potentials, there is evidence that depolarization also activates a more persistent sodium current in many central neurons. Such a current probably underlies the tetrodotoxin (TTX)-sensitive component of the anomalous rectification that has been observed in hippocampal neurons (Hotson et al., 1979; Benardo et al., 1982; Connors and Prince, 1982) and it has been suggested that sustained voltage responses to small depolarizing currents in mammalian cerebellar and inferior olive neurons are due to the presence of a noninactivating, TTX-sensitive conductance (Llinas and Sugimori, 1980; Llinas and Yarom, 1981). More direct evidence for a persistent, TTX-sensitive current activated by depolarization has been obtained in cat neocortical neurons (Stafstrom et al., 1982, 1984, 1985).

A slowly inactivating or "persistent" sodium current has been reported in a variety of cells: squid axon (Hodgkin and Huxley, 1952; Chandler and Meves, 1970a, b; Shoukimas and French, 1980; Gilly and Armstrong, 1984), Aplysia and barnacle neurons (Colmers et al., 1982; Davis and Stuart, 1988), frog node of Ranvier (Dubois and Bergman, 1975), skeletal muscle (Almers et al., 1983; Patlak and Ortiz, 1986; Gage et al., 1989), and cardiac muscle (Patlak and Ortiz, 1985; Carmeliet, 1987; Kiyosue and Arita, 1989). In squid axon, the persistent sodium current activates at more negative potentials than the transient sodium current and hence has been called a "threshold" sodium current (Gilly and Armstrong, 1984).

The aim in these experiments was to determine the characteristics of a persistent sodium current in pyramidal hippocampal neurons, particularly its magnitude, voltage dependence, and susceptibility to inactivation. A preliminary report of some early results in hippocampal slices has appeared elsewhere (French and Gage, 1985).

METHODS

Experiments were done on neurons in slices of rat hippocampus and on dissociated neurons isolated from guinea pig hippocampal slices. In both cases, preparations were submerged in a flowing solution and the changeover time of the bath was 2–5 min. When solutions had been changed for >10 min, the flow was sometimes stopped to improve recording stability. It was occasionally possible to hold cells in slices for >1 h but more often, they were held for <30 min. Recording from dissociated cells could be maintained for up to 30–40 min (on a good day) but the seal was often lost during solution changes.

The standard extracellular solution for experiments on slices contained (in millimolar): 124 NaCl, 5 KCl, 2 CaCl$_2$, 2 MgSO$_4$, 26 NaHCO$_3$, 2 NaH$_2$PO$_4$, and 10 glucose, and had a pH of 7.3–7.4 when equilibrated with 5% CO$_2$ in O$_2$. In some later experiments on isolated neurons, solutions contained no added bicarbonate or phosphate, HEPES (10 mM) was added as a pH buffer, and the NaCl concentration was increased to 150 mM. Cadmium (0.3–1 mM) was added to the extracellular solution in most experiments in order to block calcium currents. TTX was obtained from Sigma Chemical Co. (St. Louis, MO). All experiments were done at room temperature (22–24°C).

Hippocampal Slices

Female Wistar rats, 6–10 wk old, were decapitated and the hippocampus was quickly dissected out in chilled solution (4–8°C). Transverse slices, 400 μm thick, were cut with a Macilwain tissue chopper and transferred to a holding chamber where they were left for at least 1 h before any recording was attempted. After this time, one of the slices was mounted on a nylon mesh in a superfused chamber.

Microelectrodes were usually filled with 3 M CsCl, occasionally with 3 M KCl, and had resistances of 30–70 MΩ. The membrane potential was voltage-clamped using a switching voltage-clamp device that rapidly switched between voltage-monitoring and current-passing modes (Axoclamp 1; Axon Instruments Inc., Burlingame, CA). The capacitance across the wall of the microelectrode was minimized by keeping the level of the bath solution as low as possible and it was then possible to use a switching frequency of 7–10 kHz. Signals were filtered at 500 Hz (4-pole Bessel, −3 dB) and stored digitally. Four traces were usually averaged to improve the signal-to-noise ratio. Only records from cells with an input resistance >30 MΩ and resting membrane potentials more negative than −55 mV when recorded with KCl electrodes or −30 mV when recorded with CsCl electrodes were analyzed. In some cells, there was a clear discontinuity in the current-voltage curve for the transient sodium current (see Sah et al., 1988a) but this was not seen with the much smaller persistent sodium current. Cells in which loss of voltage control was detected in this way were not used in this study.

Dissociated Cells

Male or female, adult (300–500 g) guinea pigs were killed by cervical dislocation and the brain was quickly exposed, hemisected, and dissected out into cold (4–8°C) extracellular solution with composition as above. The hemisected brain was then glued to the stage of a Vibraslice (model 752; Campden Instruments, London, UK) with cyanoacrylate glue. Sections 600 μm thick were cut through the cerebral cortex and hippocampus to produce transverse hippocampal slices. The slices were dissected free of the cortex, transferred to a dish of cold oxygenated solution and the CA1 region was isolated using fine iridectomy scissors. This piece of tissue was then further cut into two or three small pieces each ~1.5 mm square. Dissociation of cells from these pieces of tissue was achieved by use of a protocol described previously (Sah et al., 1988a), very similar to that described by Numann and Wong (1984), and cells were used within an hour or two of dissociation. When it was necessary to block calcium currents, $NaHCO_3$ in the bath solution was replaced with Tris chloride and cadmium added at a concentration of 1 mM.

Electrodes were made from borosilicate glass tubing using a modified David Kopf electrode puller and coated with Sylgard (Dow Corning Corp., Midland, MI) to within 100 μm of the tip to reduce the capacitance between the intracellular solution and grounded bath solution. Electrodes were held in an electrode holder with a side arm that allowed suction to be applied to the electrode interior. After formation of a cell-attached patch, access was gained to the interior of the cell by increasing the suction to break through the patch of membrane (Hamill et al., 1981). In early experiments in which it was of interest to measure both the transient and persistent sodium currents, the electrode was connected to the 1× head stage of an Axon 2A (Axon Instruments Inc.) switching voltage-clamp device. This technique allowed the measurement of the relatively large transient current free from the complications introduced by series resistance, but had the disadvantage of introducing more noise than a patch-clamp amplifier would. In later experiments focusing on the much smaller persistent sodium current, cells were voltage-clamped and currents were recorded using a patch-clamp amplifier (EPC-7; List Electronics, Darmstadt, FRG).

Electrodes were filled with a solution containing (in millimolar): 140 CsF, 10 NaCl, 10

HEPES-CsOH, 11 EGTA, pH 7.2 and had resistances of 1–3 MΩ. Use of fluoride instead of chloride greatly aided recording stability (Fernandez et al., 1984; Kay and Wong, 1986).

Analysis

In most experiments, records were stored digitally in the computer that was used to generate the command voltages. In all experiments with dissociated cells, depolarizing voltage steps were preceded by a small hyperpolarizing voltage step (typically 10 or 20 mV, from and back to a holding potential of −90 or −100 mV) with the same duration as the test pulse. If the leakage current was appreciable (often it was not) or if the capacity current interfered with measurement of the transient current, the current generated by the hyperpolarizing step was appropriately scaled and subtracted digitally from currents generated by depolarizing voltage steps. In addition to removing linear leakage currents, this technique had the added advantage of removing linear capacity currents. Subtraction of linear capacity and leakage currents was not done for currents from cells in slices because it was possible to select cells in which there were very small leakage currents and no attempt was made to record the amplitude of the transient currents.

In general, it was considered that the most reliable method of recording the persistent sodium current free from any contamination from other currents was to subtract records obtained after exposure to TTX from those obtained before. However, it was not possible to do this in many experiments. In slices, the effect of TTX often took >20 min to develop fully, presumably because of the time for diffusion to cells not on the surface, and cells were often not held this long. In dissociated cells, changes of solution often caused loss of cells. For these reasons, we were not able to demonstrate reversal of the effect of TTX in the same cell, although the persistent sodium current could be demonstrated in other cells after washout of TTX.

RESULTS

Neurons in Slices

In voltage-clamped pyramidal neurons in hippocampal slices, depolarizing voltage steps activate a variety of voltage- and time-dependent currents, including a transient sodium current (Sah et al., 1988a) and longer lasting calcium and potassium currents (Johnston et al., 1980; Brown and Griffith, 1983a, b; Segal and Barker, 1984; Sah et al., 1988b). It was usually not possible to control potential during the transient sodium current in these cells in slices, presumably because of currents generated at a distance from the soma on the axon or dendrites, but potential appeared to be adequately controlled 10 or 20 ms after the onset of the voltage pulse when the inward current surge had largely subsided. Results from cells in which voltage was not well controlled after this time because of "breakthrough spikes" were discarded. The holding potential for cells in slices was typically set at the potential at which the holding current was zero in order to minimize ion concentration changes that might occur if a large and prolonged holding current were necessary.

Typical currents generated by a voltage step from −56 to −36 mV in a cell in a hippocampal slice are shown in Fig. 1 A. It can be seen that at the end of the voltage step lasting 400 ms, there was a net outward current. After exposure to TTX (1 μM), the outward current became larger (Fig. 1 B), suggesting that there was a persistent inward TTX-sensitive current contributing to the net current in Fig. 1 A. Subtrac-

tion of the records obtained before and after exposure to TTX gave the amplitude and time course of this persistent TTX-sensitive inward current (Fig. 1 *C*).

Although it seemed most likely that this current was carried by sodium ions, depolarization of hippocampal CA1 neurons can generate a labile calcium current (Brown and Griffith, 1983*b*). A decrease in calcium current between records *A* and *B* could conceivably give the record in *C*. Alternatively, any increase in potassium current during the change of solutions could produce the increase in outward current in *B*. In order to avoid such uncertainties, cadmium was added to extracellular solutions at a concentration of 0.3 or 0.4 mM, which effectively blocks calcium currents in these cells (Brown and Griffith, 1983*b*; French and Gage, unpublished observations), and cells were loaded with cesium from the intracellular electrode to minimize contributions from potassium currents. Under these conditions, a persistent TTX-sensitive current was still seen. Currents recorded with a 3-M CsCl elec-
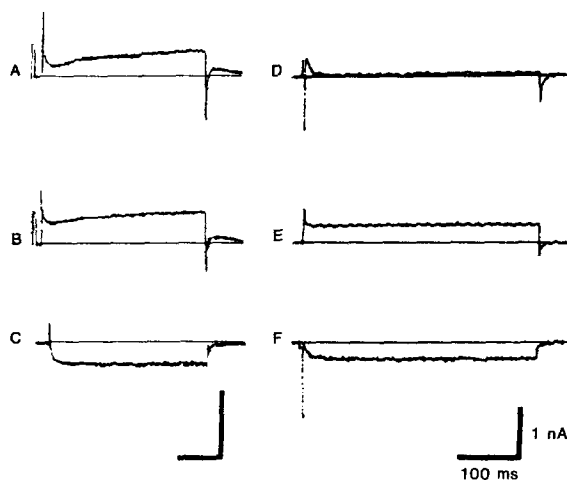

FIGURE 1. Currents recorded in voltage-clamped neurons in the CA1 region of hippocampal slices. Fast transients are not faithfully represented because records were obtained on a chart recorder with low frequency response. Subtraction of currents recorded after exposure to TTX from those recorded before reveals a persistent TTX-sensitive current. Currents in *A* and *B* were generated by voltage steps from −56 to −36 mV in control solution (*A*) and then after exposure to 1 μM TTX (*B*). Subtraction of *B* from *A* gave record *C*. Currents in *D* (control) and *E* (1 μM TTX) were generated in another neuron by voltage steps from −56 to −36 mV in solutions containing 0.3 mM cadmium to block calcium currents. Subtraction of *E* from *D* gave record *F*. Vertical calibrations, 1 nA. Horizontal calibrations, 100 ms.

trode in a solution containing 0.3 mM cadmium before exposure to TTX showed very little outward current (Fig. 1 *D*). Adding TTX to the solution removed a transient inward current and revealed a small maintained outward current (Fig. 1 *E*). Subtraction of trace *E* from trace *D* gave a transient inward current followed by a persistent inward current (Fig, 1 *F*). This result indicates that there is in these cells a genuine persistent TTX- sensitive current that does not depend on fortuitous variations in calcium or potassium currents. Nevertheless, in most of the experiments with slices reported here, the extracellular solution contained cadmium to block calcium currents and intracellular electrodes contained 3 M CsCl to block potassium currents.

Because the persistent current was an inward current at −30 to −40 mV and was blocked by TTX but not by cadmium, it was concluded that it was a sodium current.

This conclusion was supported by the observation that the amplitude of the current was reduced when the extracellular sodium concentration was lowered. For example, when extracellular sodium concentration was lowered to 40 mM in three cells, the persistent inward current was reduced on average by 0.25 nA. It was not possible to determine the change in reversal potential because of the unfavorable signal-to-noise ratio with the small residual persistent current, but the large decrease in the current with reduction in extracellular sodium concentration is a strong indication that it is indeed a sodium current.

Subtraction of currents recorded over a range of potentials before and after exposure to TTX was used to obtain current-voltage curves for the persistent
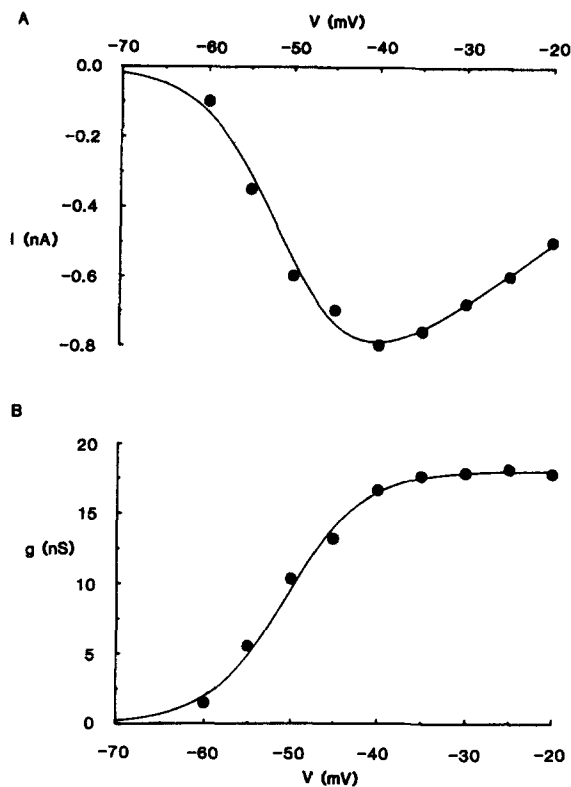

FIGURE 2. (A) The current-voltage relationship for persistent sodium currents obtained by subtraction of traces recorded before and after exposure to TTX in the neuron with the largest persistent sodium current amplitude in slices (holding potential, −65 mV). (B) The conductance-voltage curve obtained by converting the currents in A to conductance (see text). The line shows the best fit of Eq. 1 to the data points (g_{max} = 17 nS, V' = −51 mV, k = 4 mV).

sodium current in 21 neurons in slices. (In 20 of the 21 neurons, contributions from calcium currents were avoided by adding cadmium [0.3–0.4 mM] to extracellular solutions.) The typical relationship between the amplitude of the persistent sodium current and potential is illustrated in Fig. 2 A. These currents, generated from a holding potential of −65 mV, were the largest seen in any of the 21 cells. There was a significant persistent sodium current at −60 mV which increased in amplitude with further depolarization to reach a maximum of −0.76 nA at −40 mV. Linear extrapolation of the falling limb of the curve at less negative potentials (−35 to −20 mV) gave a null potential of +8 mV. (It was not found possible to record currents at potentials more positive than −20 mV because of current-pass-

ing limitations of the technique.) Because the holding potential for zero holding current was −65 mV, it was not possible to explore potentials more negative than this value in this cell. A similar voltage dependence of the current was seen in the 20 other cells that were studied. The maximum current amplitude in the 21 cells occurred at −40 mV and had an average value of −0.34 ± 0.05 nA (mean ± 1 SEM).

Currents were converted to conductance (g) for each neuron by dividing by the clamped membrane potential minus the null potential obtained by linear extrapolation. Conductances calculated from the currents in Fig. 2 *A* are plotted against clamp potential in Fig. 2 *B*. The solid line through the data points is the best (least-squares) fit to the data points of the Boltzmann equation:

$$g = g_{max}/\{1 + \exp[(V' − V)/k)]\} \tag{1}$$

where g_{max} is the maximum conductance, V' the potential at which the conductance is half-maximal, and k is a constant. The g_{max}, V', and k values for the curve in Fig. 2 *B* were 17.0 nS, −51 mV, and 4 mV respectively. The maximum average conductance (measured at −10 mV) was 7.8 ± 1.1 nS (mean ± 1 SEM, n = 21). To determine the average voltage dependence of this conductance, results from each cell were given equal weighting by expressing conductance as a fraction of the maximum conductance in that cell. The best fit of Eq. 1 to the average normalized conductance-voltage curve was obtained with values for V' and k of −49 and 5 mV, respectively.

Experiments on cells in slices were not entirely satisfactory for a variety of reasons such as: (*a*) The existence of an extensive dendritic tree raises questions about the possible contribution of currents from inadequately clamped dendritic membrane. (*b*) It is never possible to be sure that solution changes in the vicinity of a cell not on the surface are complete because of unknown diffusion delays in the tissue. (*c*) The necessity to use high resistance electrodes to minimize cell damage limits their current-carrying capacity so that the available well-clamped membrane potential range is limited and it is often not possible to control potential during larger currents. (*d*) Application of agents such as cesium to the inside of the cell to block unwanted ionic currents is limited by the fine diameter of the electrode tip. We therefore did similar experiments on dissociated cells to avoid the above problems.

Dissociated Cells

Activation of persistent sodium currents. Voltage-dependent currents were recorded in acutely dissociated (Numann and Wong, 1984; Sah et al., 1988*a*, *b*) hippocampal neurons using whole-cell tight-seal voltage-clamp techniques (Hamill et al., 1981). Inward currents were recorded over a range of potentials in 10 dissociated cells. In all of them, depolarization activated both a transient and a persistent inward current at negative clamp potentials. Typical records are shown in Fig. 3 at low (*A* and *C*) and high (*B* and *D*) gain (capacity and leakage currents have been subtracted as described in the Methods). The currents in Fig. 3, *A* and *B* were generated by a voltage step to −30 mV from a holding potential of −100 mV, and the currents in *C* and *D* by a voltage step to −10 mV from the same holding potential. With such voltage pulses, there was typically a relatively large, transient, inward cur-

rent followed by a persistent inward current. This persistent inward current can be seen more clearly in the amplified traces in B and D, in which the transient current goes off scale. The persistent inward current was not a current through calcium channels because the extracellular solution contained 1 mM cadmium.

Both the transient inward current and the persistent inward current could be blocked with TTX. The transient and persistent inward currents shown in Fig. 3 E (from a different cell than in A–D) were generated by a voltage step from a holding potential of −100 to −40 mV. After exposure to TTX (1 μM), both currents were essentially abolished (Fig. 3 F). The sensitivity to TTX and persistence in the presence of high concentrations of cadmium indicate that the persistent inward current is a sodium current corresponding to the persistent sodium current seen in the neurons in slices.
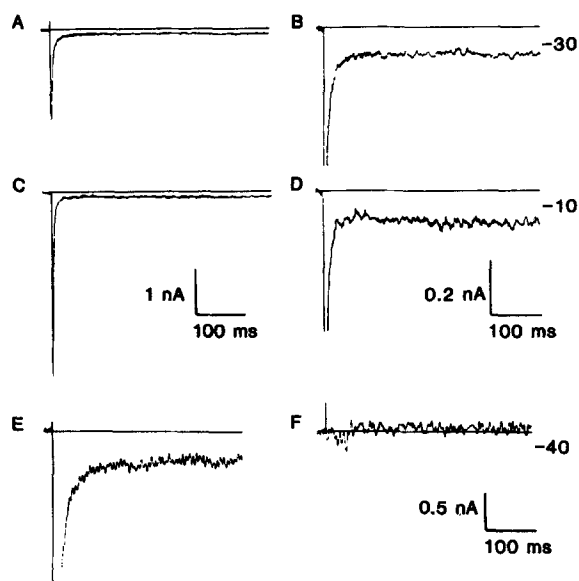

FIGURE 3. (A–D) Current traces recorded in neurons dissociated from the CA1 region of hippocampal slices. Currents were generated by voltage steps from a holding potential of −100 to −30 mV in A and B and to −10 mV in C and D. Traces in B and D are the same as in A and C except they are shown at higher gain to make the sustained currents more prominent. Vertical calibrations: 1 nA for A and C, 0.2 nA for B and D. Horizontal calibrations: 100 ms. (E and F) Current traces recorded in response to voltage pulses from −100 to −40 mV in another neuron before (E) and after (F) exposure to TTX. Vertical calibration, 0.5 nA. Horizontal calibration, 100 ms.

A family of sodium currents recorded in another cell (in an extracellular solution containing 1 mM cadmium) is shown in Fig. 4. It can be seen that there was an appreciable persistent sodium current at −70 mV that increased to −0.11 nA at −30 mV. The current-voltage relationship for the persistent sodium currents in Fig. 4 can be seen in Fig. 5 A. The current became obvious between −80 and −70 mV and reached a peak at ~−30 mV. The null potential obtained by linear extrapolation of the curve between −30 and +10 mV was +45 mV. In the 10 cells, the maximum average inward current of −0.21 ± 0.05 nA occurred at −40 mV.

Conductance, calculated from the currents in Fig. 5 A by dividing by the clamped membrane potential minus the null potential, is plotted against potential in Fig. 5 B.
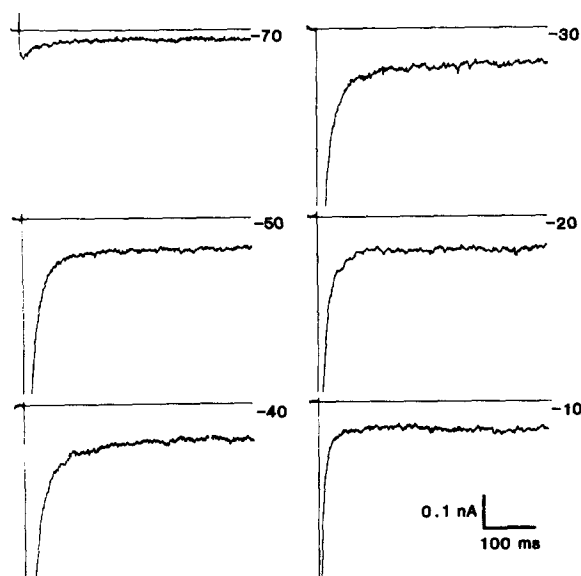
FIGURE 4. A family of persistent sodium currents generated in another dissociated neuron by voltage steps from a holding potential of −100 mV to the potentials shown alongside each trace. Vertical calibration, 0.1 nA. Horizontal calibration, 100 ms.
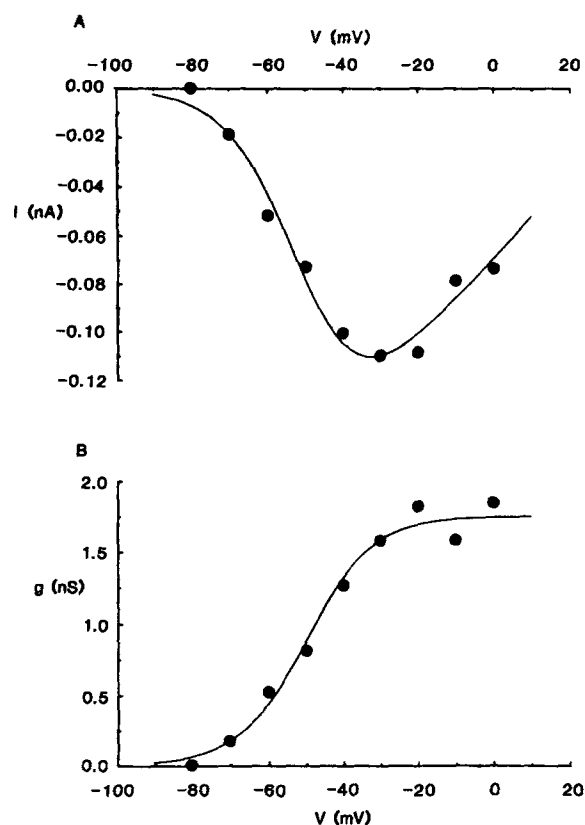

FIGURE 5. Voltage dependence of the persistent sodium current in a dissociated neuron. (A) Current amplitude at the end of 500-ms voltage pulses from a holding potential of −100 mV plotted against the potential during the pulse. (B) Conductance calculated from the current amplitudes in A plotted against clamp potential. The line shows the best fit of Eq. 1 to the data points (g_{max} = 1.75 nS, V' = −50 mV, k = 9 mV)

The solid line through the data points, the best fit of Eq. 1 to the data, was generated with a g_{max} of 1.3 nS, a V' of -50 mV, and k of 8 mV. In the 10 neurons, the average value of the maximum conductance was 4.4 ± 1.6 nS (measured at -10 mV). The best fit of Eq. 1 to the average conductance-voltage curve, obtained with conductances normalized to the maximum conductance in each cell as before, gave values for V' and k of -50.0 and 9 mV, respectively. In six of the cells, the surface area was estimated from cell input capacity assuming a specific membrane capacity of 1 μF.cm^{-2}. The average specific g_{max} calculated from these areas was 1.7 ± 0.6 pS.μm^{-2}.

Inactivation. The time course of the persistent sodium currents such as those shown in Fig. 5 indicated that the current was not inactivating appreciably during periods as long as 500 ms. The susceptibility of the persistent current to inactivation was explored further by examining the effects of varying levels of conditioning depolarization. Results obtained in one of these experiments are shown in Fig. 6. The voltage protocol is illustrated in Fig. 6 B. A 200-ms test pulse to -30 mV was
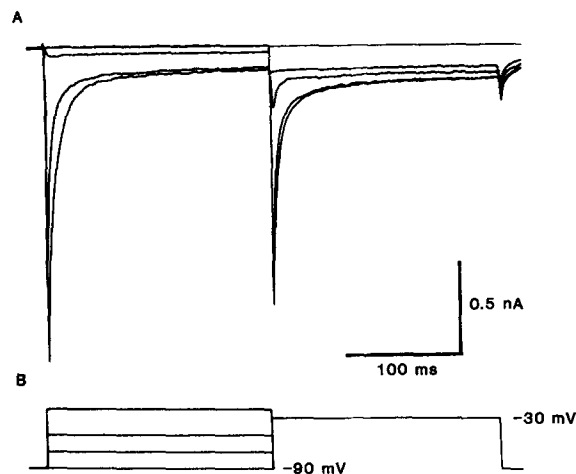

FIGURE 6. Persistent sodium currents are more resistant to conditioning depolarization than transient currents. Sodium currents (*A*) were generated by 200-ms voltage steps to -30 mV after conditioning depolarizing pulses of 0, 20, 40, and 70 mV (*B*) from a holding potential of -90 mV. Records were obtained by subtraction of corresponding currents generated before and after exposure to 10^{-7} M TTX.

preceded by 200-ms conditioning pulses to -90, -70, -50, and -20 mV. There was substantial activation of both transient and persistent currents during the prepulses to -50 and -20 mV. The transient inward current generated by the test pulse was progressively depressed by the prepulses to -70, -50, and -20 mV so that, after the prepulse to -20 mV, there was essentially no transient current. In contrast, the conditioning pulses caused much less depression of the persistent sodium current which was still of appreciable, though diminished, amplitude after the -20-mV conditioning pulse. This can be seen even more clearly in Fig. 7 A in which the currents are shown at higher gain. The amplitudes of the transient current (*filled circles*) and the persistent current (*filled triangles*) are shown plotted against conditioning potential in Fig. 7 C. The lines through the points are drawn according to:

$$I = I_{max}/\{1 + \exp [(V - V')/k)]\} \tag{2}$$

For the transient current, V' was -60 mV and k was 7 mV. With conditioning potentials from -90 to -70 mV, there was very little decrease in amplitude of the persistent current. After conditioning potentials of -30 to -20 mV, the persistent current was $\sim60\%$ of control whereas the transient current was essentially abolished. The line fitted to the persistent current amplitudes was arbitrarily calculated by assuming that 60% of the current did not inactivate and that 40% of the current obeyed Eq. 2 with $V' = -49$ mV and $k = 9$ mV.

It is clear from these results that the ratio of the amplitudes of the persistent and transient currents was not constant: it increased greatly when the amplitude of the transient current was decreased by a preceding depolarization.

Because pulses that completely inactivate the transient sodium current leave a significant part of the persistent current intact, use was made of appropriate conditioning pulses to record persistent currents separate from the transient current. The
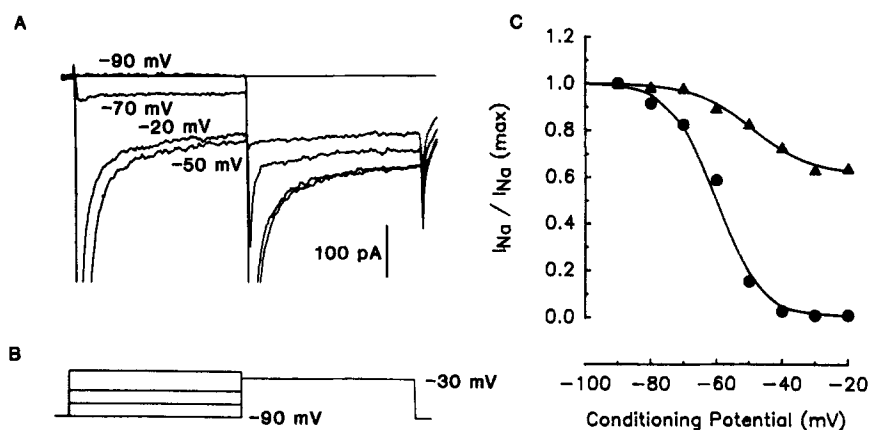

FIGURE 7. (A) Currents in Fig. 6 shown at higher gain to illustrate the amount of inactivation of the persistent current. (B) The voltage protocol used. (C) The amplitudes of the transient (*circles*) and persistent (*triangles*) sodium currents generated by a voltage pulse from -90 to -30 mV normalized to the amplitude obtained without a prepulse $[I_{Na}/I_{Na}(max)]$ are plotted against prepulse potential. The lines were fitted to the data points as described in the text.

records shown in Fig. 8 A were generated by voltage pulses to the levels shown after a conditioning pulse to -40 mV from a holding potential of -100 mV. The voltage protocol is shown in Fig. 8 B. The persistent currents recorded in this way had the same voltage dependence as the persistent currents recorded without conditioning prepulses. The change in persistent current with voltage is shown graphically in Fig. 9 A and the conductance-voltage curve is shown in Fig. 9 B. The line through the points in Fig. 9 B was drawn according to Eq. 1 with V' of -54 mV and k of 9 mV, close to the average values of -50 and 9 mV obtained when the transient current was not inactivated with a conditioning depolarization.

Prolonged, small depolarizing currents generate trains of action potentials in CA1 pyramidal cells, as illustrated in Fig. 10 A. It has been proposed that noninactivating inward currents are responsible for this kind of repetitive firing in cortical (Staf-
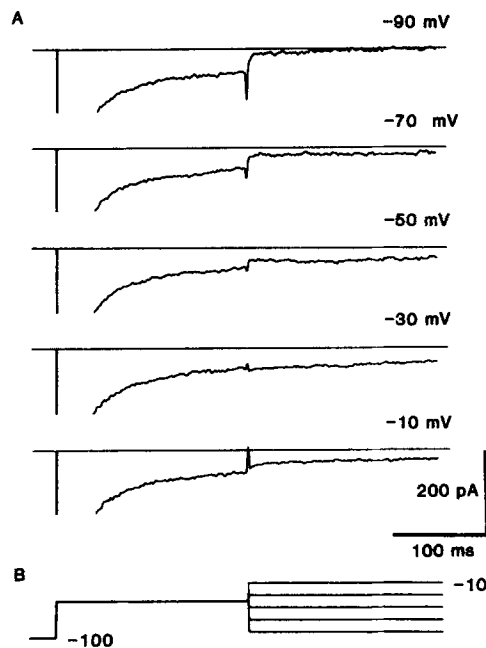
FIGURE 8. Persistent currents recorded after inactivation of the transient current with a conditioning prepulse. (A) The traces show persistent currents generated by test pulses to −90 to −10 mV after a 200-ms conditioning prepulse to −40 mV from a holding potential of −100 mV that effectively eliminated the transient current. B illustrates the voltage pulse protocol used. The records were obtained by subtraction of traces obtained before and after exposure to TTX.
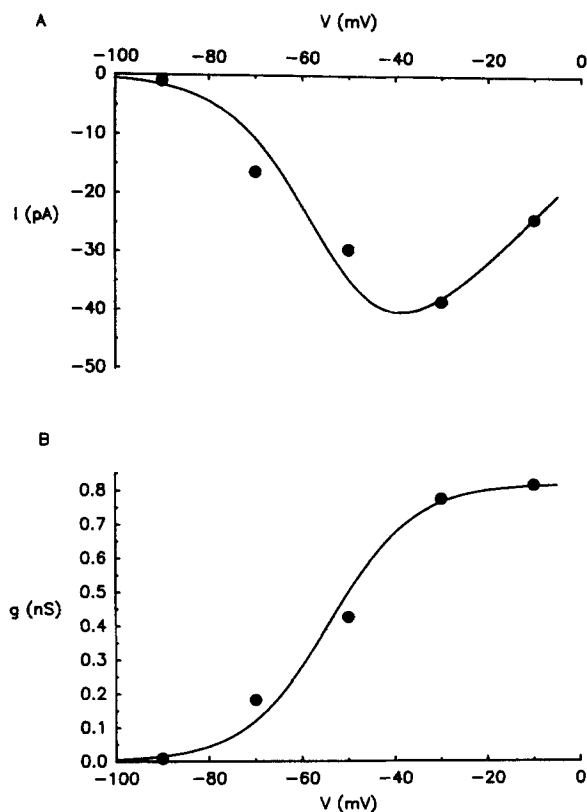

FIGURE 9. (A) The current-voltage curve obtained from the experiment illustrated in Fig. 8. The line through the points was calculated from the conductances given by the Boltzmann fit in B. (B) The corresponding conductance-voltage curve. The line was the best fit of Eq. 1 to the data with a g_{max} of 820 nS, V' of −54 mV, and k of 9 mV.

strom et al., 1984, 1985) and hippocampal (Lanthorn et al., 1984) neurons. As the repetitive firing in Fig. 10 *A* was recorded in a solution containing 1 mM cadmium, a calcium current was clearly not essential for maintaining the phenomenon. However, reducing the extracellular sodium concentration did suppress the repetitive firing as illustrated in Fig. 10 *B* in which the records were obtained after replacing 50% of the extracellular sodium chloride with Tris chloride. The sodium concentration was clearly still high enough to maintain an action potential and several action potentials could be elicited by increasing current intensity.
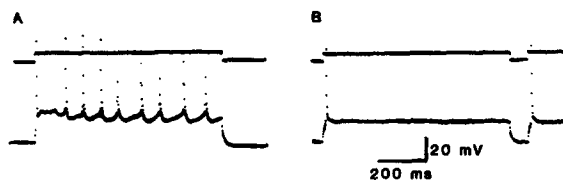
FIGURE 10. Action potentials generated by 700-ms current pulses (*upper traces*) in a neuron in a slice perfused (*A*) with control solution (see Methods) and (*B*) with a solution containing half the normal sodium concentration plus sucrose to maintain unchanged osmolarity. Solutions contained 1 mM cadmium chloride and the resting membrane potential was −56 mV in both solutions. The sampling rate was insufficient to accurately reproduce the time course of the action potentials but the repetitive firing is nevertheless clear.

DISCUSSION

In the experiments described in this paper, a relatively small, TTX-sensitive sodium current lasting several hundreds of milliseconds was recorded in pyramidal neurons from the CA1 region of rat and guinea pig hippocampus, both in cells in slices and in dissociated cells. Because of the less controlled situation in slices, the uncertainties of perfect voltage control posed by the dendritic tree, and the presence of currents other than the persistent sodium current, we place less weight on the quantitative results obtained in the slice than on results obtained in dissociated cells. However, the observations obtained in cells in slices are invaluable because they show that the persistent sodium current is not an artefact introduced by the whole-cell internal perfusion technique. The persistent sodium current, although small, is undoubtedly very important and probably plays a crucial role in the generation of bursts of action potentials caused by maintained synaptic depolarization of these cells.

A possible explanation for the persistent sodium current is that it is a "window" current arising from overlap of the steady-state inactivation and activation curves for sodium conductance (Attwell et al., 1979; Colatsky, 1982). Indeed, there is some overlap in these curves in dissociated neurons (Sah et al., 1988*a*). However, the existence of a window current depends on the assumption that the decay of transient currents is caused by the inactivation that can be measured with the steady-state inactivation curve, rather than by some different process. Such an assumption is now open to serious question (Aldrich et al., 1983; Aldrich and Stevens, 1987). Nevertheless, we have calculated the amplitude and voltage dependence of the average hypothetical window current by using the V' and k values from the Boltzmann fits to the inactivation and activation curves for the transient sodium current (Sah et

al., 1988a) in order to see if our results could be accounted for by the overlap of the activation and inactivation curves. The calculated window conductance, expressed as a fraction of the maximum transient conductance, is plotted against membrane potential in Fig. 11 A (*broken line*). The solid line shows the average persistent sodium conductance expressed as a fraction of the maximum average transient sodium conductance. It can be seen that the window current would disappear at more positive potentials where the persistent conductance was at its maximum
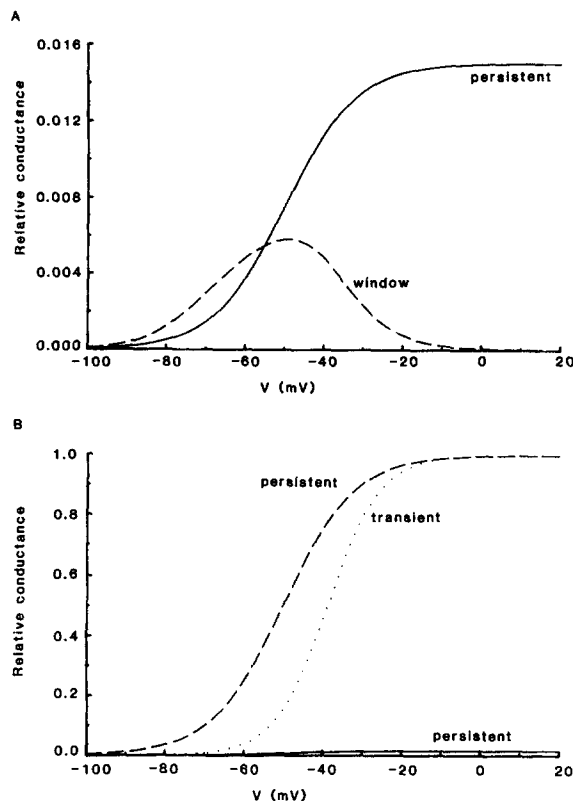

FIGURE 11. All curves are based on the best Boltzmann fits to averaged experimental data obtained in dissociated neurons and show conductance plotted against membrane potential (V). (A) Comparison of the hypothetical "window" conductance (*broken line*), calculated from inactivation and activation curves for the transient sodium current in dissociated neurons (Sah et al., 1988a), and the persistent sodium conductance recorded in dissociated neurons (*solid line*). Conductance is expressed as a fraction of the maximum transient sodium conductance. (B) Comparison of the amplitude and voltage dependence of the transient sodium conductance and persistent sodium conductance. The solid line close to the abscissa shows persistent sodium conductance expressed as as a fraction of the maximum transient sodium conductance. The dotted line shows transient sodium conductance, also expressed as a fraction of the maximum transient sodium conductance. The dashed line shows persistent sodium conductance, normalized to its own maximum value to illustrate the different voltage dependences of the persistent and transient sodium conductances.

(although, at potentials more negative than ~ −40 mV, a window current could make a significant contribution to the persistent current). A persistent current would be generated at more positive potentials, however, if the steady-state inactivation value does not become zero at these potentials, but this is the same as saying that a small fraction of channels do not inactivate at any potential, i.e., they are different from other sodium channels. Other properties of the persistent current make it unlikely that it is a simple window current.

The activation and inactivation characteristics of the persistent current are very different from those of the transient current recorded in the same cells under the same conditions.

Activation. The persistent current is activated at more negative potentials than the transient sodium current. In dissociated cells, we report here that the voltage at which the persistent sodium conductance is half-maximum is -50 mV whereas we have reported previously that half-maximal transient sodium conductance occurs at -39 mV (Sah et al., 1988a). This difference in voltage dependence of activation of the two sodium conductances is illustrated in Fig. 11 *B* in which normalized, average conductance-voltage curves for the transient current (*dotted line*: data from Sah et al., 1988a) and the persistent current in dissociated cells (*broken line*) are plotted together. The difference is also illustrated by the observation that at -70 mV, only a small fraction, if any, of the transient current is activated whereas a significant fraction of the maximum persistent current is turned on (Figs. 4, 6, and 7). A similar difference in the voltage dependence of "threshold" and transient sodium currents has also been seen in squid axon (Gilly and Armstrong, 1984).

Inactivation. The persistent current is more resistant to inactivation than the transient current. Whether the persistent current, or some part of it, is completely resistant to inactivation if depolarization is maintained indefinitely has not been determined, but it is clear that a substantial fraction of the inward current is still flowing at the end of depolarizations lasting up to 400 ms (Figs. 1, 3, 4, 6, 7 and 8). The current appeared more resistant to inactivation in the cells in slices than in dissociated cells. It is possible that some persistent sodium current arrives after a delay from regions of membrane electrically distant from the soma (e.g., on axon or dendrites) and sums with a slowly inactivating current, thus obscuring some inactivation. Alternatively, the slow inactivation that is seen in dissociated cells may be associated with the internal perfusion with cesium or fluoride ions.

The nature of the channels contributing to the persistent current remains unclear. "Late" opening sodium channels recorded during prolonged depolarization in cardiac and skeletal muscle (Patlak and Ortiz, 1985, 1986) appear to be of two kinds, the first consisting of channels transiently reopening from the inactivated state and the second of channels in which inactivation is markedly delayed. Because the transient and late single-channel currents had a similar amplitude and reversal potential and the frequency of occurrence of the late single-channel currents was correlated with the amplitude of the transient current, it was concluded by Patlak and Ortiz (1986) that the transient and late currents were generated by the same channel. We find, however, that the relationship between the amplitudes of the persistent and transient currents can vary over a wide range, i.e., there is no constant relationship between them. Indeed, it was possible to elicit an appreciable persistent current with little or no preceding transient current (Figs. 4, 6, 7, and 8), suggesting that the persistent current did not arise from a set percentage of "transient" sodium channels that did not inactivate after activation. Our observations are more consistent with the idea that the persistent current arises from channels that are very similar to the transient sodium channels but differ in their voltage sensitivity and susceptibility to inactivation. It is interesting in this context that sodium currents recorded in oocytes after injection of the high molecular weight fraction of mRNA

from rat or rabbit brain that encodes the α subunit show much slower inactivation and develop steady-state inactivation at more positive potentials (by at least 10 mV) than channels expressed after injection of unfractionated mRNA that presumably also encodes β subunits (Krafte et al., 1988). Single-channel recording revealed that the delayed inactivation was due to late openings of channels during prolonged depolarizations rather than to a change in open time. It may be that the channels responsible for the persistent current described here may lack a subunit possessed by transient channels.

The channels generating the persistent current would appear to be most densely aggregated at the soma. The average maximum conductance in 21 cells in slices was 7.8 ± 1.1 nS compared with 4.4 ± 1.6 nS in 10 dissociated cells (±1 SEM). Considering the enormous loss of membrane area during dissociation when the dendritic tree and axon are largely lost, it seems safe to conclude that at least half of the channels generating the persistent current are on or near the soma. The fraction may well be greater if intracellular perfusion depresses the persistent current. Even so, their average density must be very low. In six of the dissociated cells, surface area was estimated from the input capacity assuming a specific membrane capacity of 1 μF.cm^{-2}. The average specific g_{max} of 1.7 ± 0.6 pS.μm^{-2} for the persistent sodium current is only a small fraction (1.5%) of the specific g_{max} of 113 ± 11.6 pS.μm^{-2} for the transient sodium current, as illustrated in Fig. 11 B. If the conductance of the channels contributing to the persistent sodium conductance is assumed to be ~18 pS, the sodium channel conductance found in some other cells (Sigworth and Neher, 1980; Stuhmer et al., 1987), and all of them contribute to the maximum conductance, there must be on average about 1 persistent sodium channel per 10 μm^2 of membrane in the dissociated cells.

The rate of increase in conductance with potential was less steep in the dissociated neurons (k = 9 mV) than in neurons in situ in slices (k = 5 mV). There could be several reasons for such a discrepancy. Firstly, the dissociation procedure or internal perfusion may directly change the slope of the conductance-voltage curve. Alternatively, if there is a window current, it may be relatively larger in the dissociated cells than in the slices, either because of the more negative holding potential or more overlap in the activation and inactivation curves in the dissociated cells. By adding to the current at the more negative potentials, it would tend to decrease the slope of the conductance-voltage curve. It is also possible that a dendritic component of the persistent current might result in an artefactually steep activation. No matter what the reason for the difference in the slope of the conductance-voltage curves in neurons in slices and in dissociated neurons, a sustained current was clearly activated at potentials close to the resting membrane potential under both conditions.

In spite of the relative paucity of channels resistant to inactivation, the very high input resistance of the neurons would probably allow the small persistent sodium current to depolarize the membrane sufficiently to activate the much larger transient sodium conductance. The average current of 0.34 nA in cells in situ would cause a depolarization of >15 mV in a cell with a 50 MΩ or greater input resistance, sufficient to initiate action potentials.

Whatever the nature of the underlying channels, it would seem that the current

has all the attributes needed to generate the prepotentials seen during repetitive firing in these cells (Lanthorn et al., 1984) and in other neurons (Llinas and Sugimori, 1980; Llinas and Yarom, 1981). Small sustained subthreshold depolarizations as may occur with a barrage of asynchronous synaptic inputs (Granit et al., 1963) would activate the persistent sodium channels leading to a self-regenerative depolarization towards the threshold potential.

It is tempting to speculate, in conclusion, that alterations in expression or incorporation of specific subunits in sodium channels in a neuron may modify the amplitude of persistent sodium currents and hence influence the response of the neuron to synaptic inputs.

REFERENCES

Aldrich, R. W., D. P. Corey, and C. F. Stevens. 1983. A reinterpretation of mammalian sodium channel gating based on single channel recording. *Nature.* 306:436–441.

Aldrich, R. W., and C. F. Stevens. 1987. Voltage dependent gating of single sodium channels from mammalian *Neuroblastoma* cells. *Journal of Neuroscience.* 7:418–431.

Almers, W., P. R. Stanfield, and W. Stuhmer. 1983. Slow changes in currents through sodium channels in frog muscle membrane. *Journal of Physiology.* 339:253–271.

Atwell, D., D. Cohen, M. Eisner, M. Ohba, and C. Ojeda. 1979. The steady state TTX-sensitive ("window") sodium current in cardiac Purkinje fibres. *Pflügers Archiv.* 379:137–142.

Benardo, L. S., L. M. Masukawa, and D. A. Prince. 1982. Electrophysiology of isolated hippocampal pyramidal dendrites. *Journal of Neuroscience.* 2:1614–1622.

Brown, D. A., and W. H. Griffith. 1983a. Calcium activated outward currents in voltage clamped hippocampal neurones of the guinea pig. *Journal of Physiology.* 337:287–301.

Brown, D. A., and W. H. Griffith. 1983b. Persistent slow inward calcium current in voltage-clamped hippocampal neurones of the guinea pig. *Journal of Physiology.* 337:303–320.

Carmeliet, E. 1987. Slow inactivation of the sodium current in rabbit cardiac Purkinje fibres. *Pflügers Archiv.* 408:18–26.

Chandler, W. K., and H. Meves. 1970. Evidence for two types of sodium conductance in axons perfused with sodium fluoride solution. *Journal of Physiology.* 211:653–678.

Colatsky, T. J. 1982. Mechanisms of action of lidocaine and quinidine on action potential duration in rabbit cardiac Purkinje fibres. An effect on steady state sodium currents? *Circulation Research.* 50:17–27.

Colmers, W. F., D. V. Lewis, Jr., and A. W. Wilkie. 1982. Cs^+ loading reveals Na^+-dependent persistent inward current and negative slope resistance region in *Aplysia* giant neurons. *Journal of Neurophysiology.* 48:1191–1200.

Connors, B. W., and D. A. Prince. 1982. Effects of local anaesthetic QX-314 on the membrane properties of hippocampal pyramidal neurons. *Journal of Pharmacology and Experimental Therapeutics.* 200:476–481.

Davis, R. E., and A. E. Stuart. 1988. A persistent, TTX-sensitive sodium current in an invertebrate neuron with neurosecretory ultrastructure. *Journal of Neuroscience.* 8:3978–3991.

Dubois, J. M., and C. Bergman. 1975. Late sodium current in the node of Ranvier. *Pflügers Archiv.* 357:145–148.

Fernandez, J., A. P. Fox, and S. Krasne. 1984. Membrane patches and whole-cell membranes: a comparison of electrical properties in rat clonal pituitary (GH₃) cells. *Journal of Physiology.* 356:565–585.

French, C. R., and P. W. Gage. 1985. A threshold sodium current in pyramidal cells in rat hippocampus. *Neuroscience Letters.* 56:289–293.

Gage, P. W., G. D. Lamb, and B. T. Wakefield. 1989. Transient and persistent sodium currents in normal and denervated mammalian skeletal muscle. *Journal of Physiology.* 418:427–439.

Gilly, W. F., and C. M. Armstrong. 1984. Threshold channels—a novel type of sodium channel in squid giant axon. *Nature.* 309:448–450.

Granit, R., D. Kernell, and G. K. Shortess. 1963. The behavior of mammalian motoneurones during long-lasting orthodromic, antidromic and transmembrane stimulation. *Journal of Physiology.* 169:911–931.

Hamill, O. P., A. Marty, A. Neher, B. Sakmann, and F. Sigworth. 1981. Improved patch clamp techniques for high-resolution current recordings from cells and cell-free membrane patches. *Pflügers Archiv.* 391:85–100.

Hodgkin, A. L., and A. F. Huxley. 1952. The dual effect of membrane potential on sodium conductance in the giant axon of *Loligo. Journal of Physiology.* 116:497–506.

Hotson, J. R., D. A. Prince, and P. A. Schwartzkroin. 1979. Anomalous inward rectification in hippocampal neurons. *Journal of Neurophysiology.* 42:889–895.

Johnston, D., J. L. Hablitz, and W. A. Wilson. 1980. Voltage clamp discloses slow inward current in hippocampal burst-firing neurones. *Nature.* 286:391–393.

Kay, A. R., and R. K. S. Wong. 1986. Isolation of neurones suitable for patch-clamping from adult mammalian central nervous systems. *Journal of Neuroscience Methods.* 16:227–238.

Kiyosue, T., and M. Arita. 1989. Late sodium current and its contribution to action potential configuration in guinea pig ventricular myocytes. *Circulation Research.* 64:389–397.

Krafte, D. S., T. P. Snutch, J. P. Leonard, N. Davidson, and H. A. Lester. 1988. Evidence for the involvement of more than one mRNA species in controlling the inactivation process of rat and rabbit brain Na channels expressed in *Xenopus* oocytes. *Journal of Neuroscience.* 8:2859–2868.

Lanthorn, T., J. Storm, and P. Anderson. 1984. Current-to-frequency transduction in CA1 hippocampal pyramidal cells: slow prepotentials dominate the primary range firing. *Experimental Brain Research.* 53:431–443.

Llinas, R., and M. Sugimori. 1980. Electrophysiological properties of in vitro Purkinje cell somata in mammalian cerebellar slices. *Journal of Physiology.* 305:171–195.

Llinas, R., and Y. Yarom. 1981. Electrophysiology of mammalian inferior olivary neurones in vitro. Different types of voltage dependent ionic conductances. *Journal of Physiology.* 315:549–567.

Numann, R. E., and R. K. S. Wong. 1984. Voltage-clamp study of GABA response desensitization in single pyramidal cells dissociated from the hippocampus of adult guinea pigs. *Neuroscience Letters.* 47:289–295.

Patlak, J., and M. Ortiz. 1985. Slow currents through single sodium channels of the adult rat heart. *Journal of General Physiology.* 86:89–104.

Patlak, J. B., and M. Ortiz. 1986. Two modes of gating during late Na⁺ channel currents in frog sartorius muscle. *Journal of General Physiology.* 87:305–326.

Sah, P., A. J. Gibb, and P. W. Gage. 1988a. The sodium current underlying action potentials in guinea pig hippocampal CA1 neurons. *Journal of General Physiology.* 91:373–398.

Sah, P., A. J. Gibb, and P. W. Gage. 1988b. Potassium current activated by depolarization of dissociated neurons from adult guinea pig hippocampus. *Journal of General Physiology.* 92:263–278.

Segal, M., and J. L. Barker. 1984. Rat hippocampal neurons in culture: potassium conductances. *Journal of Neurophysiology.* 51:1409–1433.

Shoukimas, J. J., and R. J. French. 1980. Incomplete inactivation of sodium current in nonperfused squid axon. *Biophysical Journal.* 32:857–862.

Sigworth, F. J., and E. Neher. 1980. Single Na⁺ channel currents observed in cultured rat muscle cells. *Nature.* 287:497–499.

Stafstrom, C. E., P. C. Schwindt, M. C. Chubb, and W. E. Crill. 1985. Properties of persistent sodium conductance and calcium conductance of Layer V neurons from cat sensormotor cortex in vitro. *Journal of Physiology.* 53:163–170.

Stafstrom, C. E., P. C. Schwindt, and W. E. Crill. 1982. Negative slope conductance due to a persistent subthreshold sodium current in cat neocortical neurons in vitro. *Brain Research.* 236:221–226.

Stafstrom, C. E., P. C. Schwindt, and W. E. Crill. 1984. Repetitive firing in Layer V neurons of cat neocortex in vitro. *Journal of Neurophysiology.* 52:264–277.

Stuhmer, W., B. Methfessel, B. Sakmann, M. Noda, and S. Numa. 1987. Patch clamp characterization of sodium channels expressed from rat brain cDNA. *European Biophysics Journal.* 14:131–138.

Author/s:
FRENCH, CR; SAH, P; BUCKETT, KJ; GAGE, PW

Title:
A VOLTAGE-DEPENDENT PERSISTENT SODIUM CURRENT IN MAMMALIAN
HIPPOCAMPAL-NEURONS

Date:
1990-06-01

Citation:
FRENCH, CR; SAH, P; BUCKETT, KJ; GAGE, PW, A VOLTAGE-DEPENDENT
PERSISTENT SODIUM CURRENT IN MAMMALIAN HIPPOCAMPAL-NEURONS,
JOURNAL OF GENERAL PHYSIOLOGY, 1990, 95 (6), pp. 1139 - 1157

Persistent Link:
http://hdl.handle.net/11343/240379

File Description:
Published version